https://doi.org/10.5194/acp-2020-203
Preprint. Discussion started: 16 March 2020

Atmospheric Chemistry and Physics Discussions

Glyoxal's impact on dry ammonium salts: fast and reversible surface aerosol browning

David O. De Haan,*[1] Lelia N. Hawkins,[2] Kevin Jansen,[3] Hannah G. Welsh,[2] Raunak Pednekar,[2,5] Alexia de Loera,[1] Natalie G. Jimenez,[1] Margaret A. Tolbert,[3] Mathieu Cazaunau,[4] Aline Gratien,[4] Antonin Bergé,[4] Edouard Pangui,[4] Paola Formenti,[4] Jean-François Doussin[4]

[1] Department of Chemistry and Biochemistry, University of San Diego, 5998 Alcala Park, San Diego CA 92110 USA
[2] Department of Chemistry, Harvey Mudd College, 301 Platt Blvd, Claremont CA 91711 USA
[3] Department of Chemistry / Cooperative Institute for Research in Environmental Sciences, University of Colorado, Boulder CO 80309 USA
[4] Laboratoire Interuniversitaire des Systèmes Atmosphériques (LISA), UMR7583, CNRS, Université Paris-Est-Créteil (UPEC) et Université de Paris, Institut Pierre Simon Laplace (IPSL), Créteil, France
[5] Deceased

Correspondence to: David O. De Haan (ddehaan@sandiego.edu)

Abstract. Alpha-dicarbonyl compounds are believed to form brown carbon in the atmosphere via reactions with ammonium sulfate (AS) in cloud droplets and aqueous aerosol particles. In this work, brown carbon formation in AS and other aerosol particles was quantified as a function of relative humidity (RH) during exposure to gas-phase glyoxal (GX) in chamber experiments. Under dry conditions (RH < 5%), solid AS, AS/glycine, and methylammonium sulfate aerosol particles brown within minutes upon exposure to GX, while sodium sulfate particles do not. When GX concentrations decline, browning goes away, demonstrating that this dry browning process is reversible. Declines in aerosol albedo are found to be a function of $[GX]^2$, and are consistent between AS and AS/glycine aerosol. Dry methylammonium sulfate aerosol browns 4× more than dry AS aerosol, but deliquesced AS aerosol browns much less than dry AS aerosol. Optical measurements at 405, 450, and 530 nm provide an estimated Ångstrom absorbance coefficient of -16 ±4. This coefficient and the empirical relationship between GX and albedo are used to estimate an upper limit to global radiative forcing by brown carbon formed by 70 ppt GX reacting with AS ($+7.6 \times 10^{-5}$ W/m^2). This quantity is < 1% of the total radiative forcing by secondary brown carbon, but occurs almost entirely in the ultraviolet range.

1 Introduction

Brown carbon is the name given to light-absorbing organic molecules present in atmospheric aerosol. Estimates of the global direct radiative effect of brown carbon aerosol range from +0.05 to 0.27 W/m^2 (Tuccella et al., 2020;Laskin et al., 2015;Zhang et al., 2019;Wang et al., 2018). This absorption occurs mainly at ultraviolet (UV) and near-UV wavelengths, suppressing photochemistry in areas with high loadings (Mok et al., 2016). Limiting emissions of brown carbon aerosol and its precursor

https://doi.org/10.5194/acp-2020-203
Preprint. Discussion started: 16 March 2020


Atmospheric Chemistry and Physics Discussions

species could provide immediate climate benefits. Approximately 30% of brown carbon is secondary (Mukai and Ambe, 1986;Hecobian et al., 2010), formed from gas-phase species often through reactions taking place in clouds, fog, and aqueous aerosol particles (Hecobian et al., 2010). Reactions between small, multi-function aldehydes such as glyoxal and ammonium salts (Shapiro et al., 2009;Kampf et al., 2012), and oxidation reactions of phenolic species (Chang and Thompson, 2010) are two examples of aqueous-phase brown carbon formation processes.

Glyoxal uptake to deliquesced ammonium sulfate particles is rapid (Kroll et al., 2005), but is difficult to detect on dry aerosol (Corrigan et al., 2008). Glyoxal reacts to form brown carbon imidazole derivatives in solutions containing ammonium ions (Shapiro et al., 2009;Noziere et al., 2009;Galloway et al., 2009;Yu et al., 2011;Kampf et al., 2012;Maxut et al., 2015) or primary amine species such as glycine or methylamine (De Haan et al., 2009a;De Haan et al., 2009b). While in bulk aqueous solution these reactions take hours to days (Shapiro et al., 2009;Noziere et al., 2009;Powelson et al., 2014), they can occur in minutes in aqueous aerosol particles, likely due to surface reactivity of glyoxal in its monohydrate form (De Haan et al., 2009a).

In this work, we report rapid and reversible browning of dry ammonium sulfate (AS), AS/glycine, and methylammonium sulfate (MeAS) aerosol particles upon exposure to gas phase glyoxal. This browning process is not accompanied by appreciable particle growth, and is reversed upon addition of water vapor.

2 Methods

2.1 Large chamber experiments

CESAM is a 4.2 m^3 temperature- and pressure-controlled, stirred, stainless steel chamber (Wang et al., 2011) with solar simulator lamps (Harris et al., 2017), held just above ambient pressure with automated flows of high purity O_2 and liquid N_2 boil-off at a respective 20/80 v/v ratio. The chamber gas phase contents were monitored by a relative humidity (RH) sensor (Vaisala HMP234 Humicap), long-path FTIR spectroscopy (Bruker Tensor 37, 182.5 ±0.5 m path length (Wang et al., 2011), glyoxal integrated 2950-2700 cm^{-1} band intensity = 6.34 $\times 10^{-18}$ cm $molec^{-1}$ (Eurochamp, 2010)), and high-resolution proton transfer reaction mass spectrometry (PTR-MS, KORE Tech. Series II, inlet temperature 100°C, proton transfer reactor P = 1.64 mbar, glow discharge P = 1.94 mbar, PTR entry voltage = 400 V, E/N ratio = 130). Polydisperse seed particles (TSI 3076 atomizer) were diffusion dried before addition to the dry chamber, then continuously sampled through a 1 m Nafion drying tube to scanning mobility particle sizing (SMPS, TSI, 20 – 900 nm) and cavity-attenuated phase shift single-scattering albedo (450 nm CAPS-ssa, Aerodyne) (Onasch et al., 2015) spectrometers. A particle-into-liquid sampler (PILS, Brechtel Manufacturing) sampled N_2-diluted chamber aerosol through an activated carbon denuder, into a capillary waveguide UV/vis spectrometer (LWCC-100, 0.94m pathlength). Water vapor was added in bursts from a stainless steel boiler (Wang et al., 2011), and chamber RH was subsequently stabilized by routing inlet N_2 flow through a heated high-purity water bubbler. A

https://doi.org/10.5194/acp-2020-203
Preprint. Discussion started: 16 March 2020


Atmospheric Chemistry and Physics Discussions

droplet spectrometer (Palas Welas Digital 2000, 0.5 to 15 μm diam., on chamber flange) (Wang et al., 2011) extended the size range of detected aerosol into supermicron particles. CAPS-ssa aerosol extinction and scattering signals were zeroed against filtered chamber air every 5 min to ensure that any gas-phase species absorbing light at 450 nm do not influence measurements, and averaged to SMPS scan frequency. SMPS number and concentrations and PTR-MS signals were corrected for dilution caused by flows into the chamber. SMPS size distributions were also corrected for wall losses.

2.2 Small chamber experiments

Additional experiments were conducted in a 300 L collapsible Tedlar chamber. Aerosols were generated from 0.1% w/w aqueous solutions (TSI 3076 atomizer) and diffusion dried (except in experiments on "wet" aerosol). Glyoxal production was monitored at the inlet by absorbance at 405 nm using a cavity ringdown (CRD) spectrometer and a cross section of 4.491×10^{-20} cm^2 $molecule^{-1}$ (Volkamer et al., 2005b). Glyoxal concentrations at the chamber outlet were measured in test experiments to determine wall loss rates (~6.7×10^{-4} s^{-1}). Glyoxal inlet concentrations, flow mixing ratios, and wall loss rates were then used to estimate glyoxal chamber concentrations. Aerosol particles were sampled via diffusion driers by Q-AMS (Aerodyne), CAPS-ssa (Aerodyne, 450 nm), SMPS (TSI), CRD (530 nm) (Ugelow et al., 2017), and photoacoustic spectrometers (PAS, 405 and 530 nm) (Ugelow et al., 2017). RH sensors monitored humidity levels at the aerosol inlet, chamber outlet, and dried chamber outlet flows. Water vapor was added in certain experiments by passing inlet flows through Nafion humidifiers.

2.3 Chemicals

Reagents were used as received from Sigma-Aldrich unless otherwise mentioned. Solutions for aerosol generation were generated by dilution of glycine (>99%) to 5 mM, AS (>99%) to 1.2 – 10 mM, or sodium sulfate (≥99%) to 7 mM in deionized water (>18 MΩ, ELGA Maxima). MeAS was generated by mixing methylamine and sulfuric acid (Mallinckrodt) solutions at a 2:1 molar ratio; after dilution to 6.3 mM, solution pH was 4.5. Gas-phase glyoxal was generated by heating solid mixtures of glyoxal trimer dihydrate (Fluka, >95%) and P_2O_5 (99%) to 110-150 °C; the glyoxal produced was flushed into the chamber with dry N_2 (Volkamer et al., 2009).

3. Results

Chamber experiments where aerosol particles were exposed to gas-phase glyoxal are summarized in Table 1.

3.1 Dry AS and AS/glycine aerosol (experiments 1-4)

Experiment 1, where dry AS aerosol was sequentially exposed to 0.05 ppm and then 0.50 ppm glyoxal at t = 4:47 and 5:16 h, respectively, is summarized in Figure 1. Both glyoxal additions were detectable by PTR-MS at *m/z* 31 and 59. (The *m/z* 59 signal, however, is elevated in the clean and dry chamber before glyoxal is added, indicating background interference by another chemical species or its fragment in the mass spectrometer.) SMPS data, which has been corrected for wall losses and for dilution, shows no observable aerosol growth after either glyoxal gas addition. This lack of growth is not surprising since

https://doi.org/10.5194/acp-2020-203
Preprint. Discussion started: 16 March 2020


Atmospheric Chemistry and Physics Discussions

the glyoxal additions occurred at <5% RH, and is consistent with the lack up uptake of α-dicarbonyl compounds observed in previous studies under very dry conditions (Kroll et al., 2005;De Haan et al., 2017).

The addition of 0.05 ppm glyoxal gas at t = 4:47 h caused detectable increases in PTR-MS signals at m/z 31 and 59. At the same time, a short-lived drop in albedo by 0.034 was observed by CAPS-ssa at 450 nm. A second larger glyoxal addition (0.50 ppm) at t = 5:16 h produced much greater increases in gas-phase glyoxal PTR-MS signals, and a sudden albedo decrease to 0.75. Over the next 30 minutes, glyoxal gas-phase concentrations decreased by half. Since SMPS data shows that particles were not detectably growing during this time (rather, aerosol mass declined by 5%), this loss of gas-phase glyoxal must have been largely to the steel chamber walls. However, the large albedo decline without particle growth indicates that at least some glyoxal is causing browning reactions at dry particle surfaces. As gas-phase glyoxal concentrations declined, albedo recovered proportionately, indicating that this surface brown carbon formation under dry conditions is reversible.

When the chamber was humidified to 50% RH, a level which would not deliquesce the AS seeds (Biskos et al., 2006) but which may cause measurable water uptake by AS (Denjean et al., 2014) or glyoxal reaction products (Hawkins et al., 2014), significant changes were observed in both the gas and aerosol phases (at t = 5:46 in Figure 1). Glyoxal PTR-MS signals and aerosol albedo returned within a few minutes back to near-baseline levels, while the dried aerosol mass measured by SMPS jumped downward by 15%. The albedo recovery and SMPS mass loss suggest that humidification destroys the light-absorbing products of the "dry browning" process residing at the solid aerosol surface, converting some fraction of them to gas-phase products. (It is significant that no browning was observed in PILS-sampled aerosol in experiment 1, presumably due to the same destruction of "dry browning" products by water during sampling.) Simultaneous increases in gas-phase PTR-MS signals for m/z 47 (formic acid) and 61 (acetic acid) indicate that these acids are two of the gas-phase products generated by humidification. Formic acid is a known byproduct of imidazole production by aqueous-phase glyoxal + ammonia reactions (De Haan et al., 2009a;Yu et al., 2011).

Dried seed aerosol particles atomized from AS-glycine mixtures were also exposed to 0.25 ppm glyoxal under dry conditions in experiment 2 (Figure S1). The response of these internally mixed seeds to glyoxal exposure was comparable to that of pure AS seeds. No growth was observed by SMPS, and aerosol albedo at 450 nm was anticorrelated with PTR-MS glyoxal signals at m/z 59, as before. The most significant difference between the experiments is that there was no 15% loss of aerosol mass observed by SMPS upon humidification of the chamber to 50% RH, even though acetic and formic acid were again released into the gas phase. This may be due to the lower volatility of deprotonated seed particle materials (glycine vs. ammonia).

To better understand the reactive processes happening in the dry aerosol particles, further experiments were conducted in a 300 L Tedlar chamber probed by Q-AMS, CAPS-ssa, and CRD/PAS. Figure S2 shows an AMS ion correlation plot comparing signals before and after 40 ppb glyoxal was added to the dry chamber containing AS aerosol in experiment 3. The addition of

https://doi.org/10.5194/acp-2020-203
Preprint. Discussion started: 16 March 2020


Atmospheric Chemistry and Physics Discussions

this smaller amount of glyoxal did not cause an observable decline in aerosol albedo at 450 nm, but increases in aerosol-phase ion signals were observed in multiple experiments at *m/z* 15 (CH_3^+ or NH^+ fragments), 23 (Na^+), and 69 (protonated imidazole), while slight decreases in aerosol water signals were observed at *m/z* 16. Increases were seen in single experiments at *m/z* 29 (CHO^+ fragment), 47 (formic acid $+H^+$), 97 and 119 (imidazole carboxyaldehyde "IC" $+H^+$ and Na^+, respectively).) The presence of particle phase imidazole, formic acid, and IC suggests that larger, light-absorbing molecules such as 2,2'-biimidazole that are typically associated with the products detected here (Kampf et al., 2012) may also be present. However, detection of these larger product molecules directly from dry aerosol may require a soft, direct ionization technique such as extractive electrospray ionization (EESI-) MS.

The anticorrelation of albedo with glyoxal concentrations in experiments 1-4 is summarized in Figure 2. Although AS-glycine-glyoxal aqueous mixtures have been shown to brown more than mixtures without glycine (Trainic et al., 2012;Powelson et al., 2014), here we see that dry AS and AS/glycine aerosol particles brown similarly for a given concentration of gas-phase glyoxal. This may indicate that glycine is not at the aerosol surface, or that glycine surfaces, when present, are less able to retain adsorbed water in the dry chamber. We therefore fit the combined dataset from all 4 experiments. Albedo shows a clear downward curvature at high glyoxal concentrations, such that the relationship is best fit by a 2nd order polynomial. This suggests that the formation of the compounds absorbing at 450 nm is proportional to [glyoxal]^2.

Reversible surface browning of AS aerosol under dry conditions was also recently observed during exposures to methylglyoxal gas (De Haan et al., 2017). The albedo values observed before and after two methylglyoxal additions are shown for comparison in Figure 2. Although the data shows a slight negative offset due to particle size effects, judging by the slope it is clear that methylglyoxal's effect on the albedo of dry AS aerosol is significantly less than glyoxal. This is the opposite of the trend in brown carbon production in bulk aqueous solutions at pH 5, where methylglyoxal is much more effective in generating light-absorbing products (Powelson et al., 2014), perhaps due to the fact that its ketone functional group is far less likely to be inactivated by hydration than the aldehyde groups on both molecules. However, in these dry aerosol experiments where water is scarce, glyoxal's greater attraction to water (seen in its much higher Henry's law coefficient) (Betterton and Hoffmann, 1988;Ip et al., 2009;Kampf et al., 2013) may allow it to interact with small amounts of adsorbed water at the AS aerosol surface far more effectively than methylglyoxal.

3.2 Dry MeAS or sodium sulfate aerosol (experiments 8 - 9)

Gas phase glyoxal was added to a few other types of seed particles in the small chamber. In experiments on MeAS seeds (expt. 8, Figure 3 top panel), the slow addition of 140 ppb of glyoxal caused a matching drop of -0.15 in aerosol albedo measured by CAPS-ssa at 450 nm and an increase in aerosol absorbance to 28 Mm^{-1} measured by PAS at 405 nm. The albedo decline at 450 nm (Figure 2, green circles) is 4× greater than observed on AS seeds at similar glyoxal concentrations. This

https://doi.org/10.5194/acp-2020-203
Preprint. Discussion started: 16 March 2020


Atmospheric Chemistry and Physics Discussions

result is consistent with earlier aqueous-phase studies showing greater browning in glyoxal – methylamine mixtures than in glyoxal – AS mixtures at the same pH (Powelson et al., 2014).

Albedo at 405 nm was calculated from PAS and CRD signals in expt. 8 (Figure S3), showing that albedo had dropped to 0.30 by 1:11 pm and remained at this level for 45 minutes. These albedo values indicate that maximum light absorbance at 405 nm was 4.7× greater than at 450 nm, and persisted for a longer period of time after glyoxal gas concentrations decline. At even longer wavelengths (530 nm), PAS aerosol absorbance reached only 0.9 Mm^{-1}, further indicating highly wavelength-dependent light absorption. The absorption spectra of atmospheric brown carbon are typically well-fit by exponential decay functions. Such featureless spectra can be characterized by an Ångstrom absorption coefficient α, which is the slope of a log(absorbance) vs log(wavelength) plot. Comparing the amount of light absorbance at 405, 450, and 530 nm at 1:11 pm in experiment 8 gives α = -12.7 ±0.8 (Figure S5). A similar analysis of expt. 4 (Figures S6 and S7, dry AS + glyoxal), the only other experiment with measurable absorbance at all 3 wavelengths, gives a comparable α = -16 ±4. Thus, it appears that brown carbon formed by glyoxal under dry conditions on AS and MeAS aerosol absorb light with similar wavelength dependence.

In an experiment on dry sodium sulfate seeds at ~35% RH in the small Tedlar chamber (expt. 9, Figure 3) glyoxal concentrations were increased from zero to ~2000 ppb over 30 min. During this time, albedo at 450 nm remained at 1 ±0.005, and no aerosol absorbance was measured by PAS at either 530 or 405 nm. The lack of browning observed even at such high glyoxal concentrations confirms that ammonium or methylammonium ions (or ammonia or methylamine) are necessary reaction partners with glyoxal in the browning process observed in experiments 1-4 and 8. It also confirms that our CAPS and PAS measurements are not biased by absorbance due to gas-phase glyoxal.

3.3 Deliquesced AS aerosol (experiments 5-7)

Finally, three experiments exploring browning on wet rather than dry AS aerosol were conducted at RH ranging from 38 to 81%. In the three experiments, albedo declines of 0.013 or less were observed following addition of 0.12, 1.1, and 1.2 ppm of glyoxal gas, respectively. If graphed in Figure 2, the resulting slopes for experiments 6-7 would be more than 1000x flatter than the methylglyoxal data shown for comparison. While some of the glyoxal gas added may have been quickly lost to the walls of the humid chambers as an equilibrium is established (Kroll et al., 2005), especially in experiments 5-6, it is clear that wet AS aerosol particles brown much less than dry AS, AS/glycine, or MeAS aerosol upon exposure to glyoxal.

Enhanced AS aerosol browning under dry conditions is surprising, given that glyoxal Maillard chemistry is normally considered an aqueous-phase process. One clue to the nature of the dry browning process is seen in the slight depletion of water signals observed in all dry experiments probed by Q-AMS (#3, 4, 8, Figures S2 and S8) after browning caused by glyoxal exposure. (Most water is removed from aerosol particles in the AMS inlet.) The extra water depletion associated with glyoxal

https://doi.org/10.5194/acp-2020-203
Preprint. Discussion started: 16 March 2020


Atmospheric Chemistry and Physics Discussions

exposure of dry aerosol, which was not observed in deliquesced aerosol experiments probed by Q-AMS (#6-7), suggests that even under dry conditions, glyoxal is able to access and deplete trace amounts of aerosol-phase surface water. Any adsorbed water would be saturated with ammonium (or methylammonium) sulfate, and the presence of dissolved AS is known to greatly increase glyoxal uptake via a "salting in" effect (Kampf et al., 2013;Waxman et al., 2015), while methylglyoxal solubility is reduced by salting out (Waxman et al., 2015). In a previous study, similar reasoning was used to explain glyoxal uptake on solid seed particles at RH levels as low as 10% (Corrigan et al., 2008). Furthermore, the scarcity of water will favor dehydration of products, helping to form light-absorbing conjugated double bonds.

4 Discussion

Since methylglyoxal is generally less abundant in the atmosphere than glyoxal (Igawa et al., 1989;Munger et al., 1995;Matsumoto et al., 2005), and since the browning of dry AS by methylglyoxal is much less than that of glyoxal likely due to salting effects (Kampf et al., 2013;Waxman et al., 2015), we will focus on the effects of instantaneous browning of atmospheric aerosol particles due to interaction with glyoxal. We will assume that all tropospheric sulfate particles contain ammonium, and, as an upper limit, that tropospheric sulfate particles would brown as much as the pure AS particles used in this study regardless of the presence of additional aerosol species. The first assumption is generally reasonable (Jimenez et al., 2009), since acidic sulfate aerosol takes up ammonia in the atmosphere, while the second assumption will clearly result in the estimation of an upper limit, since the presence of other materials at aerosol particle surfaces has been shown to limit the extent of the interactions between glyoxal and ammonium ions (Drozd and McNeill, 2014). While few locations in the troposphere are as dry as in this study, tropospheric aerosol is nevertheless typically semi-solid or solid phase, except low over the Amazon and Arctic (Shiraiwa et al., 2017).

Using the albedo = $-0.97[GX]^2 - 0.16[GX] + 1.00$ function from Figure 2, a global 24-h average glyoxal concentration of ~70 ppt (Fu et al., 2008;Zhou and Mopper, 1990b;Zhou and Mopper, 1990a;Munger et al., 1995;Spaulding et al., 2003;Matsunaga et al., 2004;Müller et al., 2005;Ieda et al., 2006) would lower particle albedo at 450 nm ($\Delta Albedo(450)$) by only 1.1×10^{-5}. Using our measured Ångstrom absorption coefficient $\alpha = -16$ for glyoxal + AS brown carbon formed under dry conditions, we estimated albedo depression at other wavelengths ($\Delta Albedo(\lambda)$) between 280 and 4000 nm using Eq. (1):

$$\frac{\log\left(\frac{\Delta Albedo(\lambda)}{\Delta Albedo(450)}\right)}{\log\left(\frac{\lambda}{450}\right)} = \alpha \quad (1)$$

These albedo decreases were multiplied by the solar spectrum (ASTM G173-03) times the wavelength-dependent scattering function of AS aerosol (Nemesure et al., 1995) at each wavelength (Figure S9), and then integrated across the spectrum. 97%

https://doi.org/10.5194/acp-2020-203
Preprint. Discussion started: 16 March 2020


Atmospheric Chemistry and Physics Discussions

of the solar energy absorbed by this brown carbon source is predicted to be in the UV range, with the absorbed energy peaking near 330 nm. The total fraction of energy absorbed by glyoxal + AS brown carbon (absorption × solar spectrum × scattering function) is calculated to be 1.9×10^{-4}, relative to the total energy scattered by AS aerosol (solar spectrum × scattering function). We then multiply this energy fraction times the magnitude of global direct radiative forcing due to sulfate scattering, estimated by the IPCC to be -0.4 ±0.2 W/m^2 (Ramaswamy et al., 2018), to quantify a global radiative forcing of $+7.6 \times 10^{-5}$ W/m^2 by dry browning of ammonium sulfate aerosol. This climate forcing is negligible compared to the global net aerosol direct effect (-0.45 ±0.5 W/m^2) or absorption by black carbon ($+0.4\ ^{+0.4}_{-0.35}$ W/m^2) (Ramaswamy et al., 2018), and is less than 1% of estimates of radiative forcing by secondary brown carbon (+0.015 to +0.081 W/m^2) (Mukai and Ambe, 1986;Hecobian et al., 2010;Shamjad et al., 2015;Tuccella et al., 2020). While dry browning of ammonium sulfate aerosol in the presence of ambient glyoxal thus does not appear to be globally significant in terms of radiative forcing, it may be regionally significant in polluted areas where glyoxal concentrations can greatly exceed 70 ppt (Volkamer et al., 2005a), where larger loadings of AS aerosol are present, or where aerosol browning by glyoxal occurs in the upper troposphere (Zhang et al., 2017).

5 Supporting Information

Supporting Information is available: data summaries of experiments 2, 4, 8, and 9, Ångstrom coefficient plots for experiments 4 and 8, Q-AMS plots summarizing the effects of glyoxal addition in experiments 3 and 8, and estimated spectrum of absorbance of sulfate-scattered solar radiation due to glyoxal uptake.

6 Acknowledgments

This work was funded by NSF grant AGS-1523178 and AGS-1826593. L. N. Hawkins was funded by the Barbara Stokes Dewey Foundation and Research Corporation (CCSA 22473). The authors thank Mila Ródenas García (CEAM) for access to the *Main Polwin* MATLAB program and for glyoxal FTIR reference spectra. CNRS-INSU is gratefully acknowledged for supporting CESAM as an open facility through the National Instrument label. The CESAM chamber has received funding from the European Union's Horizon 2020 research and innovation program through the EUROCHAMP-2020 Infrastructure Activity under grant agreement No 730997.

Data availability

Data is available from the authors upon request.

https://doi.org/10.5194/acp-2020-203
Preprint. Discussion started: 16 March 2020

Atmospheric Chemistry and Physics Discussions

Author Contributions

David De Haan guided the project and wrote the manuscript. Lelia Hawkins and Jean-François Doussin guided large chamber experiments. Margaret Tolbert guided small chamber experiments. Kevin Jansen conducted small chamber experiments. Hannah Welsh, Raunak Pednekar, Alexia de Loera, Natalie Jimenez, Mathieu Cazaunau, and Edouard Pangui conducted large chamber experiments. Aline Gratien and Antonin Bergé quantified glyoxal by FTIR in the large chamber. Paola Formenti provided assistance in interpreting optical measurements.

Competing Interests

The authors declare no competing interests.

References

Betterton, E. A., and Hoffmann, M. R.: Henry's Law constants of some environmentally important aldehydes, Environ. Sci. Technol., 22, 1415-1418, 10.1021/es00177a004, 1988.

Biskos, G., Paulsen, D., Russell, L. M., Buseck, P. R., and Martin, S. T.: Prompt deliquescence and efflorescence of aerosol nanoparticles, Atmos. Chem. Phys., 6, 4633-4642, 10.5194/acp-6-4633-2006, 2006.

Chang, J. L., and Thompson, J. E.: Characterization of colored products formed during irradiation of solutions containing H_2O_2 and phenolic compounds, Atmos. Environ., 44, 541-551, 10.1016/j.atmosenv.2009.10.042, 2010.

Corrigan, A. L., Hanley, S. W., and De Haan, D. O.: Uptake of glyoxal by organic and inorganic aerosol, Environ. Sci. Technol., 42, 4428-4433, 10.1021/es7032394, 2008.

De Haan, D. O., Corrigan, A. L., Smith, K. W., Stroik, D. R., Turley, J. T., Lee, F. E., Tolbert, M. A., Jimenez, J. L., Cordova, K. E., and Ferrell, G. R.: Secondary organic aerosol-forming reactions of glyoxal with amino acids, Environ. Sci. Technol., 43, 2818-2824, 10.1021/es803534f, 2009a.

De Haan, D. O., Tolbert, M. A., and Jimenez, J. L.: Atmospheric condensed-phase reactions of glyoxal with methylamine, Geophys. Res. Lett., 36, L11819, 10.1029/2009GL037441, 2009b.

De Haan, D. O., Hawkins, L. N., Welsh, H. G., Pednekar, R., Casar, J. R., Pennington, E. A., de Loera, A., Jimenez, N. G., Symons, M. A., Zauscher, M., Pajunoja, A., Caponi, L., Cazaunau, M., Formenti, P., Gratien, A., Pangui, E., and Doussin, J. F.: Brown carbon production in ammonium- or amine-containing aerosol particles by reactive uptake of methylglyoxal and photolytic cloud cycling, Environ Sci Technol, 51, 7458-7466, 10.1021/acs.est.7b00159, 2017.

Denjean, C., Formenti, P., Picquet-Varrault, B., Katrib, Y., Pangui, E., Zapf, P., and Doussin, J. F.: A new experimental approach to study the hygroscopic and optical properties of aerosols: application to ammonium sulfate particles, Atmos. Meas. Tech., 7, 183-197, 10.5194/amt-7-183-2014, 2014.

Drozd, G. T., and McNeill, V. F.: Organic matrix effects on the formation of light-absorbing compounds from [small alpha]-dicarbonyls in aqueous salt solution, Environmental Science: Processes & Impacts, 16, 741-747, 10.1039/C3EM00579H, 2014.

Fu, T.-M., Jacob, D. J., Wittrock, F., Burrows, J. P., Vrekoussis, M., and Henze, D. K.: Global budgets of atmospheric glyoxal and methylglyoxal, and implications for formation of secondary organic aerosols, J. Geophys. Res., 113, D15303, 10.1029/2007JD009505, 2008.

https://doi.org/10.5194/acp-2020-203
Preprint. Discussion started: 16 March 2020

Galloway, M. M., Chhabra, P. S., Chan, A. W. H., Surratt, J. D., Flagan, R. C., Seinfeld, J. H., and Keutsch, F. N.: Glyoxal uptake on ammonium sulphate seed aerosol: reaction products and reversibility of uptake under dark and irradiated conditions, Atmos. Chem. Phys., 9, 3331-3345, 10.5194/acp-9-3331-2009, 2009.

Harris, A., Cazaunau, M., Gratien, A., Pangui, E., and Doussin, J.-F.: Atmospheric Simulation Chamber Studies of the Gas-Phase Photolysis of Pyruvic Acid, The Journal of Physical Chemistry A, 121, 10.1021/acs.jpca.7b05139, 2017.

Hawkins, L. N., Baril, M. J., Sedehi, N., Galloway, M. M., De Haan, D. O., Schill, G. P., and Tolbert, M. A.: Formation of semi-solid, oligomerized aqueous SOA: Lab simulations of cloud processing, Environ Sci Technol, 48, 2273-2280, 10.1021/es4049626, 2014.

Hecobian, A., Zhang, X., Zheng, M., Frank, N., Edgerton, E. S., and Weber, R. J.: Water-soluble organic aerosol material and the light-absorption characteristics of aqueous extracts measured over the southeastern United States., Atmos. Chem. Phys., 10, 5965-5977, 10.5194/acp-10-5965-2010, 2010.

Ieda, T., Kitamori, Y., Mochida, M., Hirata, R., Hirano, T., Inukai, K. O. U., Fujinuma, Y., and Kawamura, K.: Diurnal variations and vertical gradients of biogenic volatile and semi-volatile organic compounds at the Tomakomai larch forest station in Japan, Tellus B, 58, 177-186, 10.1111/j.1600-0889.2006.00179.x, 2006.

Igawa, M., Munger, J. W., and Hoffmann, M. R.: Analysis of aldehydes in cloud- and fogwater samples by HPLC with a postcolumn reaction detector, Environ. Sci. Technol., 23, 556-561, 10.1021/es00063a007, 1989.

Ip, H. S. S., Huang, X. H. H., and Yu, J. Z.: Effective Henry's law constants of glyoxal, glyoxylic acid, and glycolic acid, Geophys. Res. Lett., 36, L01802, 10.1029/2008gl036212, 2009.

Jimenez, J. L., Canagaratna, M. R., Donahue, N. M., Prevot, A. S. H., Zhang, Q., Kroll, J. H., DeCarlo, P. F., Allan, J. D., Coe, H., Ng, N. L., Aiken, A. C., Docherty, K. S., Ulbrich, I. M., Grieshop, A. P., Robinson, A. L., Duplissy, J., Smith, J. D., Wilson, K. R., Lanz, V. A., Hueglin, C., Sun, Y. L., Tian, J., Laadsonen, A., Raatikainen, T., Rautiainen, J., Vaattovaara, P., Ehn, M., Kulmala, M., Tomlinson, J. M., Collins, D. R., Cubison, M. J., Dunlea, E. J., Huffman, J. A., Onasch, T. B., Alfarra, M. R., Williams, P. I., Bower, K., Kondo, Y., Schneider, J., Drewnick, F., Borrmann, S., Weimer, S., Demerjian, K., Salcedo, D., Cottrell, L., Griffin, R., Takami, A., Miyoshi, T., Hatakeyama, S., Shimono, A., Sun, J. Y., Zhang, Y. M., Dzepina, K., Kimmel, J. R., Sueper, D., Jayne, J. T., Herndon, S. C., Trimborn, A. M., Williams, L. R., Wood, E. C., Middlebrook, A. M., Kolb, C. E., Baltensperger, U., and Worsnop, D. R.: Evolution of organic aerosols in the atmosphere, Science, 326, 1525-1529, 10.1126/science.1180353, 2009.

Kampf, C. J., Jakob, R., and Hoffmann, T.: Identification and characterization of aging products in the glyoxal/ammonium sulfate system -- implications for light-absorbing material in atmospheric aerosols, Atmos. Chem. Phys., 12, 6323-6333, 10.5194/acp-12-6323-2012, 2012.

Kampf, C. J., Waxman, E. M., Slowik, J. G., Dommen, J., Pfaffenberger, L., Praplan, A. P., Prévôt, A. S. H., Baltensperger, U., Hoffmann, T., and Volkamer, R.: Effective Henry's Law Partitioning and the Salting Constant of Glyoxal in Aerosols Containing Sulfate, Environ Sci Technol, 47, 4236-4244, 10.1021/es400083d, 2013.

Kroll, J. H., Ng, N. L., Murphy, S. M., Varutbangkul, V., Flagan, R. C., and Seinfeld, J. H.: Chamber studies of secondary organic aerosol growth by reactive uptake of simple carbonyl compounds, J. Geophys. Res., 110, D23207, 10.1029/2005jd006004, 2005.

Laskin, A., Laskin, J., and Nizkorodov, S. A.: Chemistry of Atmospheric Brown Carbon, Chem. Rev., 115, 4335-4382, 10.1021/cr5006167, 2015.

Matsumoto, K., Kawai, S., and Igawa, M.: Dominant factors controlling concentrations of aldehydes in rain, fog, dew water, and in the gas phase., Atmos. Environ., 39, 7321-7329, 10.1016/j.atmosenv.2005.09.009, 2005.

Matsunaga, S., Mochida, M., and Kawamura, K.: Variation on the atmospheric concentrations of biogenic carbonyl compounds and their removal processes in the northern forest at Moshiri, Hokkaido Island in Japan, J. Geophys. Res., 109, D04302, 10.1029/2003JD004100, 2004.

Maxut, A., Noziere, B., Fenet, B., and Mechakra, H.: Formation mechanisms and yields of small imidazoles from reactions of glyoxal with NH4+ in water at neutral pH, Phys. Chem. Chem. Phys., 17, 20416-20424, 10.1039/C5CP03113C, 2015.

https://doi.org/10.5194/acp-2020-203
Preprint. Discussion started: 16 March 2020

Atmospheric Chemistry and Physics Discussions

Mok, J., Krotkov, N. A., Arola, A., Torres, O., Jethva, H., Andrade, M., Labow, G., Eck, T. F., Li, Z., Dickerson, R. R., Stenchikov, G. L., Osipov, S., and Ren, X.: Impacts of brown carbon from biomass burning on surface UV and ozone photochemistry in the Amazon Basin, Scientific Reports, 6, 36940, 10.1038/srep36940, 2016.

Mukai, H., and Ambe, Y.: Characterization of a humic acid-like brown substance in airborne particulate matter and tentative identification of its origin, Atmospheric Environment (1967), 20, 813-819, https://doi.org/10.1016/0004-6981(86)90265-9, 1986.

Müller, K., van Pinxteren, D., Plewka, A., Svrcina, B., Kramberger, H., Hofmann, D., Bächmann, K., and Herrmann, H.: Aerosol characterisation at the FEBUKO upwind station Goldlauter (II): Detailed organic chemical characterisation, Atmos. Environ., 39, 4219-4231, https://doi.org/10.1016/j.atmosenv.2005.02.008, 2005.

Munger, J. W., Jacob, D. J., Daube, B. C., Horowitz, L. W., Keene, W. C., and Heikes, B. G.: Formaldehyde, glyoxal, and methylglyoxal in air and cloudwater at a rural mountain site in central Virginia, J. Geophys. Res., 100, 9325-9333, 10.1029/95JD00508, 1995.

Nemesure, S., Wagener, R., and Schwartz, S. E.: Direct shortwave forcing of climate by the anthropogenic sulfate aerosol: Sensitivity to particle size, composition, and relative humidity, Journal of Geophysical Research: Atmospheres, 100, 26105-26116, 10.1029/95JD02897, 1995.

Noziere, B., Dziedzic, P., and Cordova, A.: Products and kinetics of the liquid-phase reaction of glyoxal catalyzed by ammonium ions (NH_4^+), J. Phys. Chem., 113, 231-237, 10.1021/jp8078293, 2009.

Onasch, T. B., Massoli, P., Kebabian, P. L., Hills, F. B., Bacon, F. W., and Freedman, A.: Single scattering albedo monitor for airborne particulates., Aerosol Sci. Technol., 49, 267-279, 10.1080/02786826.2015.1022248, 2015.

Powelson, M. H., Espelien, B. M., Hawkins, L. N., Galloway, M. M., and De Haan, D. O.: Brown carbon formation by aqueous-phase aldehyde reactions with amines and ammonium sulfate, Environ Sci Technol, 48, 985-993, 10.1021/es4038325, 2014.

Ramaswamy, V., Collins, W., Haywood, J., Lean, J., Mahowald, N., Myhre, G., Naik, V., Shine, K. P., Soden, B., Stenchikov, G., and Storelvmo, T.: Radiative Forcing of Climate: The Historical Evolution of the Radiative Forcing Concept, the Forcing Agents and their Quantification, and Applications, Meteorological Monographs, 59, 14.11-14.101, 10.1175/AMSMONOGRAPHS-D-19-0001.1, 2018.

Shamjad, P. M., Tripathi, S. N., Pathak, R., Hallquist, M., Arola, A., and Bergin, M. H.: Contribution of Brown Carbon to Direct Radiative Forcing over the Indo-Gangetic Plain, Environ Sci Technol, 49, 10474-10481, 10.1021/acs.est.5b03368, 2015.

Shapiro, E. L., Szprengiel, J., Sareen, N., Jen, C. N., Giordano, M. R., and McNeill, V. F.: Light-absorbing secondary organic material formed by glyoxal in aqueous aerosol mimics, Atmos. Chem. Phys., 9, 2289-2300, 10.5194/acp-9-2289-2009, 2009.

Shiraiwa, M., Li, Y., Tsimpidi, A. P., Karydis, V. A., Berkemeier, T., Pandis, S. N., Lelieveld, J., Koop, T., and Pöschl, U.: Global distribution of particle phase state in atmospheric secondary organic aerosols, Nature Communications, 8, 15002, 10.1038/ncomms15002, 2017.

Spaulding, R. S., Schade, G. W., Goldstein, A. H., and Charles, M. J.: Characterization of secondary atmospheric photooxidation products: evidence for biogenic and anthropogenic sources, Journal of Geophysical Research, [Atmospheres], 108, 4247, 10.1029/2002JD002478, 2003.

Trainic, M., Abo Riziq, A., Lavi, A., and Rudich, Y.: Role of interfacial water in the heterogeneous uptake of glyoxal by mixed glycine and ammonium sulfate aerosols, J. Phys. Chem., 116, 5948-5957, 10.1021/jp2104837, 2012.

Tuccella, P., Curci, G., Pitari, G., Lee, S., and Jo, D. S.: Direct radiative effect of absorbing aerosols: sensitivity to mixing state, brown carbon and soil dust refractive index and shape, Journal of Geophysical Research: Atmospheres, n/a, 10.1029/2019JD030967, 2020.

Ugelow, M. S., Zarzana, K. J., Day, D. A., Jimenez, J. L., and Tolbert, M. A.: The optical and chemical properties of discharge generated organic haze using in-situ real-time techniques, Icarus, 294, 1-13, https://doi.org/10.1016/j.icarus.2017.04.028, 2017.

https://doi.org/10.5194/acp-2020-203
Preprint. Discussion started: 16 March 2020

Volkamer, R., Molina, L. T., Molina, M. J., Shirley, T., and Brune, W. H.: DOAS measurement of glyoxal as an indicator for fast VOC chemistry in urban air, Geophys. Res. Lett., 32, L08806, 10.1029/2005GL022616, 2005a.

Volkamer, R., Spietz, P., Burrows, J., and Platt, U.: High-resolution absorption cross-section of glyoxal in the UV–vis and IR spectral ranges, Journal of Photochemistry and Photobiology A: Chemistry, 172, 35-46, https://doi.org/10.1016/j.jphotochem.2004.11.011, 2005b.

Volkamer, R., Ziemann, P. J., and Molina, M. J.: Secondary organic aerosol formation from acetylene (C_2H_2): seed effect on SOA yields due to organic photochemistry in the aerosol aqueous phase, Atmos. Chem. Phys., 9, 1907-1928, 10.5194/acp-9-1907-2009, 2009.

Wang, J., Doussin, J. F., Perrier, S., Perraudin, E., Katrib, Y., Pangui, E., and Picquet-Varrault, B.: Design of a new multi-phase experimental simulation chamber for atmospheric photosmog, aerosol and cloud chemistry research, Atmos. Meas. Tech., 4, 2465-2494, 10.5194/amt-4-2465-2011, 2011.

Wang, X., Heald, C. L., Liu, J., Weber, R. J., Campuzano-Jost, P., Jimenez, J. L., Schwarz, J. P., and Perring, A. E.: Exploring the observational constraints on the simulation of brown carbon, Atmos. Chem. Phys., 18, 635-653, 10.5194/acp-18-635-2018, 2018.

Waxman, E. M., Elm, J., Kurtén, T., Mikkelsen, K. V., Ziemann, P. J., and Volkamer, R.: Glyoxal and Methylglyoxal Setschenow Salting Constants in Sulfate, Nitrate, and Chloride Solutions: Measurements and Gibbs Energies, Environ Sci Technol, 49, 11500-11508, 10.1021/acs.est.5b02782, 2015.

Yu, G., Bayer, A. R., Galloway, M. M., Korshavn, K. J., Fry, C. G., and Keutsch, F. N.: Glyoxal in aqueous ammonium sulfate solutions: products, kinetics, and hydration effects, Environ. Sci. Technol., 45, 6336-6342, 10.1021/es200989n, 2011.

Zhang, A., Wang, Y., Zhang, Y., Weber, R. J., Song, Y., Ke, Z., and Zou, Y.: Modeling global radiative effect of brown carbon: A larger heating source in the tropical free troposphere than black carbon, Atmos. Chem. Phys. Discuss., 2019, 1-36, 10.5194/acp-2019-594, 2019.

Zhang, Y., Forrister, H., Liu, J., Dibb, J., Anderson, B., Schwarz, J. P., Perring, A. E., Jimenez, J. L., Campuzano-Jost, P., Wang, Y., Nenes, A., and Weber, R. J.: Top-of-atmosphere radiative forcing affected by brown carbon in the upper troposphere, Nature Geosci., 10, 486, 10.1038/ngeo2960, 2017.

Zhou, X., and Mopper, K.: Measurement of sub-parts-per-billion levels of carbonyl compounds in marine air by a simple cartridge trapping procedure followed by liquid chromatography, Environ Sci Technol, 24, 1482-1485, 10.1021/es00080a004, 1990a.

Zhou, X., and Mopper, K.: Apparent partition coefficients of 15 carbonyl compounds between air and seawater and between air and freshwater; implications for air-sea exchange, Environ. Sci. Technol., 24, 1864-1869, 1990b.

https://doi.org/10.5194/acp-2020-203
Preprint. Discussion started: 16 March 2020

Atmospheric Chemistry and Physics Discussions

Table 1: Summary of Glyoxal Gas Addition Experiments:

Expt #	[GX][a] (ppm)	aerosol type	aerosol conc. ($\mu g/m^3$)	RH at glyoxal addition (%)	mass increase ($\mu g/m^3$)	albedo change, 450 nm (rapid[b])
1a	0.05	AS	82	< 5	< 0.2	-0.034
1b	0.50	AS	82	< 5	-3 (decr)	-0.233
2	0.25	AS/Gly	78	< 5	< 1	-0.094
3[c]	0.04[d]	AS	50	< 5	0.9[e,f]	-0.001
4[c]	0.30[d]	AS	40[f]	< 5	< 1	-0.069
5	0.12[g]	wet AS	70	77	< 1.6	-0.013
6[c]	1.1[d]	wet AS	180[f]	81	< 1	-0.012
7[c]	~1.2[d]	wet AS	120	38	< 1	-0.010
8[c]	0.14[d]	MeAS	80[f]	< 5	< 1	-0.15
9[c]	2.0[d]	Na_2SO_4	70[f]	35	< 1	0

Notes: GX = glyoxal; AS = ammonium sulfate; Gly = glycine; MeAS = methylammonium sulfate. **a**: Tabulated GX concentrations are peak values measured by PTR-MS, ±20% rel. uncertainty unless otherwise stated. **b**: occurring within 5 min. of GX addition. **c**: Experiment performed in 300 L Tedlar bag. **d**: estimated from PAS measurements at chamber inlet. **e**: Organic aerosol growth. **f**: measured by Q-AMS. **g**: Estimated from addition bulb pressure and comparison of PTR-MS signals of *m/z* 72 imine product.

https://doi.org/10.5194/acp-2020-203
Preprint. Discussion started: 16 March 2020

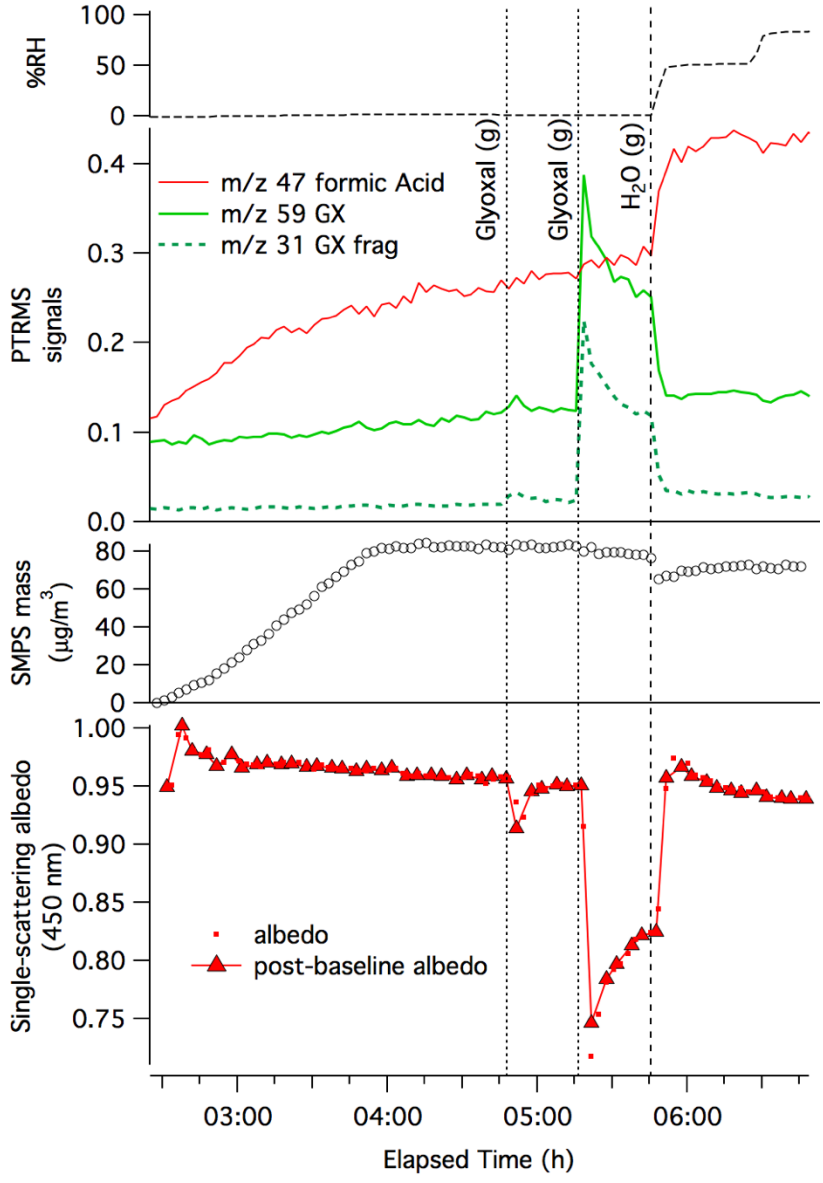

Figure 1: Pulse glyoxal addition experiment 1 on dry AS aerosol in CESAM chamber. Top: chamber RH. Middle panels: Dilution- and water-corrected PTR-MS traces for gas-phase glyoxal (*m/z* = 59, green line), a glyoxal fragment (*m/z* 31, dark green dotted line), formic acid (*m/z* 47, red line); SMPS particulate mass corrected for wall losses and dilution (assuming aerosol density = 1, open black circles), with increasing mass for first 90 minutes indicating AS aerosol addition to chamber. Bottom: single-scattering albedo (red dots), and albedo values calculated from data immediately following instrument baseline on gas-phase contents of chamber (red triangles), measured by CAPS-ssa at 450 nm. Sequential gas "(g)" additions of 0.05 and 0.50 ppm glyoxal (vertical dotted line) and water vapor addition (dashed lines) are labeled. Elapsed time is measured from start of N_2 addition to the evacuated chamber.

https://doi.org/10.5194/acp-2020-203
Preprint. Discussion started: 16 March 2020

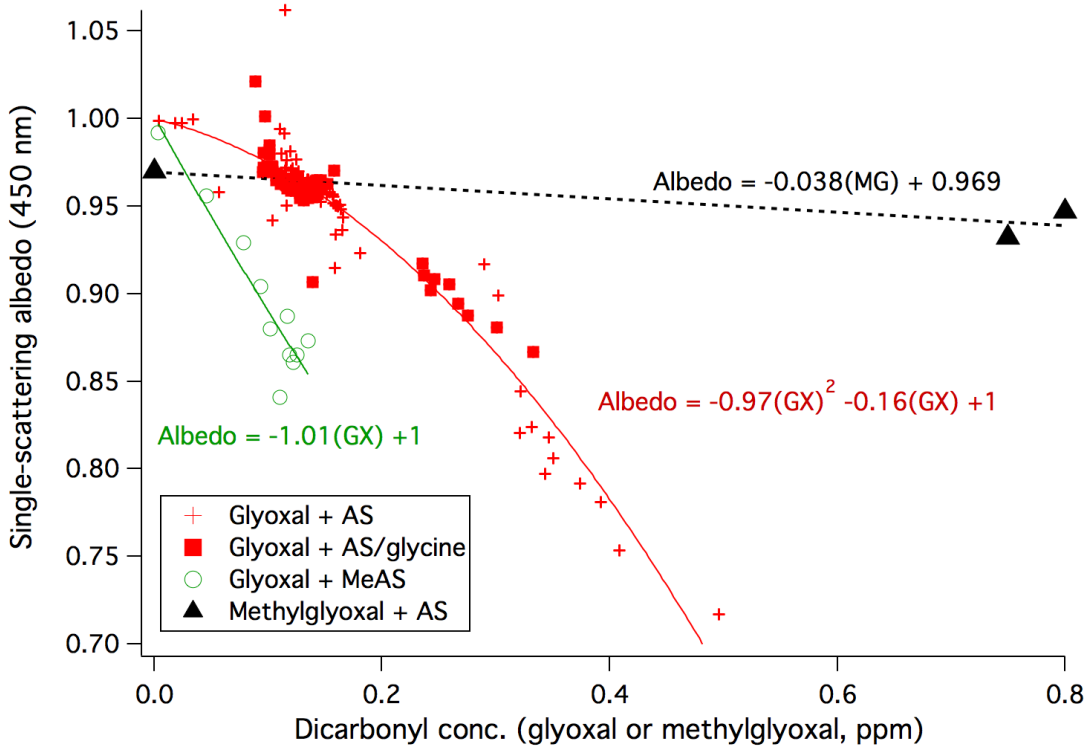

Figure 2: Top: Anticorrelation of particle single-scattering albedo at 450 nm (with a 3 – 7 min delay) with gas-phase concentrations of glyoxal (Expts. 1, 3, and 4: dry AS, red +; Expt. 2: dry AS/glycine, filled red squares; Expt. 8: dry MeAS, green circles) and methylglyoxal (black triangles, from ref (De Haan et al., 2017)) as measured by PTR-MS (expts. 1-2 and methylglyoxal data) or photoacoustic spectroscopy (expts. 3-4, 8).

https://doi.org/10.5194/acp-2020-203
Preprint. Discussion started: 16 March 2020

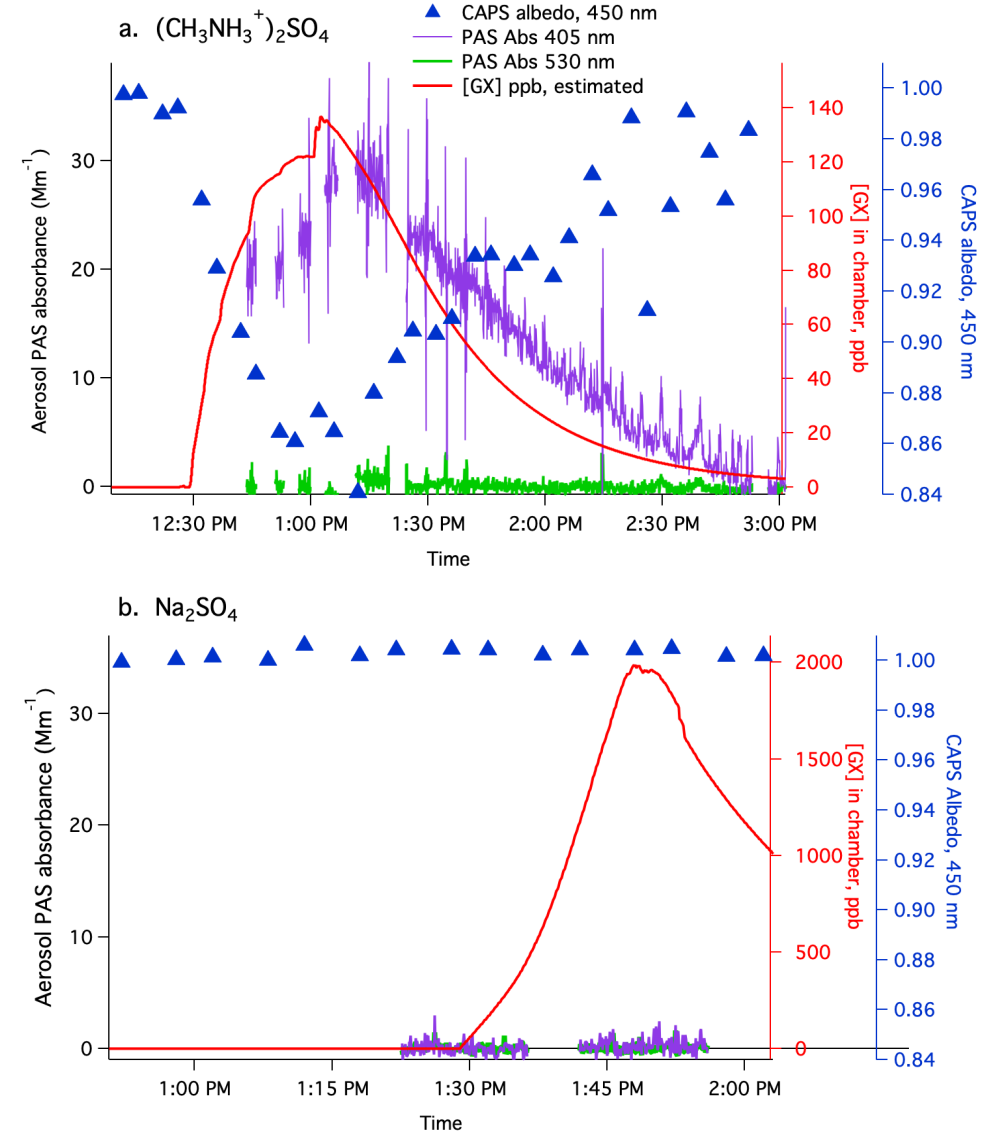

Figure 3: Gradual glyoxal addition experiments in small Tedlar chamber on **a.**) dry methylammonium sulfate aerosol (experiment 8), and **b.**) dry sodium sulfate aerosol (experiment 9). Aerosol absorbance measured by PAS at 405 nm (purple line) and 530 nm (green line), aerosol albedo measured by CAPS at 450 nm (blue triangles, blue axis), and estimated glyoxal concentrations in the chamber (red line, red axis, calculated using GX measurements at inlet, flow mixing ratios, and GX wall loss rate = 6.7×10^{-4} s^{-1}). CRD, SMPS, and 405 nm albedo data for these experiments is displayed in Figures S3 and S4, respectively.